Absolute helicity-dependent photoabsorption cross sections of Fe thin films and quantitative evaluation of magnetic-moment determination

V. Chakarian* and Y. U. Idzerda
Naval Research Laboratory, Code 6345, Washington, D.C. 20375

C. T. Chen†
AT&T Bell Laboratories, 600 Mountain Ave, Murray Hill, New Jersey 07974

(Received 6 February 1997)

Energy and helicity-dependent absolute photoabsorption cross sections at the Fe $L_{2,3}$ edge, measured in transmission from a supported ultrathin Fe film, are presented. These cross sections and semiempirical total-electron-yield (TEY) equations are used to show that the effects of saturation/self-absorption in the TEY spectra, as reflected in the quantitative evaluation of magnetic moments, can be quite severe. These conclusions are confirmed by directly comparing the data obtained simultaneously by TEY and transmission. [S0163-1829(98)08209-5]

The extraction of reliable *quantitative* results from measured x-ray-absorption spectra often requires the determination of absolute photoabsorption cross sections. Magnetic circular dichroism (MCD), a variant of x-ray-absorption spectroscopy (XAS), is a relatively new technique that relies heavily upon the determination of accurate *helicity-dependent* photoabsorption cross sections. The MCD spectra, which is the difference in the absorption of left- and right-circularly polarized photons, can be used to extract element-specific magnetic-moment information.[1–3] Such measurements allow for the determination of the orbital, $m_l=\langle L_z\rangle$, and spin, $m_s=-2\ \langle S_z\rangle$, contributions to the total magnetic moment of each constituent element.[4–9]

There are three commonly used methods for quantitative XAS measurements: transmission yield (TY), fluorescence yield (FY), and total-electron yield (TEY). The TY method is the most direct and accurate, assuming that the reflectivity is small (satisfied for nongrazing photon incidence angles), while the latter two methods are indirect and suffer from a number of artifacts. There is ample evidence that the FY method suffers from spin-dependent decay channel complications, making it unsuitable for quantitative helicity-dependent photoabsorption cross sections,[10–12] while the TEY measurements may suffer from *intrinsic* spin-dependent transmission asymmetries (as the emitted electrons traverse magnetic overlayers) and from an *extrinsic* detection efficiency imbalance due to external/stray magnetic fields. Despite their shortcomings, the indirect methods are usually preferred since the transmission method is often not practical at spectroscopically interesting soft-x-ray energies due to small photon penetration depth.

One of the major challenges in the determination of accurate XAS spectra has been the correction of the collected TEY and FY spectra for saturation and self-absorption effects (nonlinear deviations of the measured photoabsorption cross sections from the ''true'' values with effective sample thickness). The general method of extracting the correct values from the XAS spectra collected either via FY or TEY is to use semiempirical, phenomenological yield equations to correct the measured spectra.[7–11,13,14] In these corrected spectra, even small deviations from the actual absorption cross sections may result in significant errors in the extracted quantities that require energy integration of the XAS or MCD spectra, as is required for magnetic-moment determination.

In this article, we present experimental helicity-dependent XAS (and hence MCD) spectra, measured *simultaneously* in transmission and in TEY. We show conclusively that, even in cases where traditional XAS line shape based criteria suggest the effects to be minimal, the saturation/self-absorption effects can indeed be severe in MCD. We begin by presenting a method to directly determine *absolute helicity-dependent* photoabsorption cross sections at the L edges of the $3d$ transition metals from transmission measurements and use it to determine the corresponding cross sections for bcc Fe. Second, utilizing these experimental cross sections combined with a semiempirical, phenomenological description of TEY, we calculate the anticipated XAS and MCD spectra to illustrate the extent to which saturation/self-absorption effects alter the measured TEY spectra. Finally, we compare the experimental TEY results to our calculations.

(1). *Determination of absolute helicity-dependent photoabsorption cross sections*. The TY method, while the most straightforward for determining the energy-dependent photoabsorption cross sections, is the most difficult, since at these soft-x-ray energies employed in transition metal studies, the photons have a very small penetration depth. For this reason, the magnetic material and the underlying substrate must be sufficiently transparent to allow significant transmission of the incident flux. This can be accomplished by either preparing free-standing magnetic films of <200 Å thick, or by depositing a thin magnetic film onto a suitable substrate which is mechanically strong but is relatively transparent with featureless absorption spectrum in the energy regions of interest. Since free-standing, high-purity films of this thickness are difficult to manufacture, the use of a supportive substrate, a $\sim 1\ \mu$m-thick semitransparent parylene, $(C_8H_8)_n$, was preferred for this study.

The experiments were conducted at the NRL/NSLS U4B

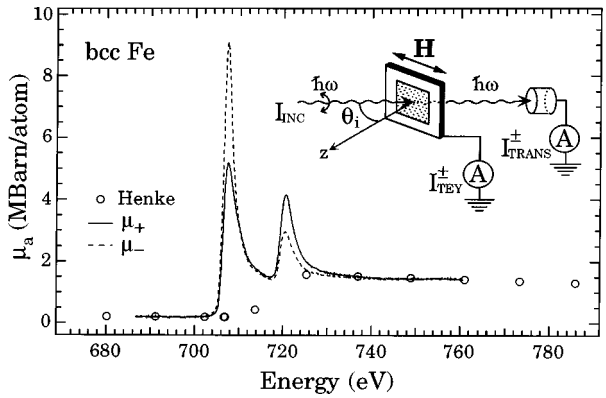

FIG. 1. Absolute μ_+ and μ_- for Fe thin film, normalized as described in text to the published tables of cross sections (symbols). The inset shows the experimental arrangement.

beamline at the National Synchrotron Light Source.[15,16] The Fe films were deposited *in situ* at 10^{-10} Torr pressure from *e*-beam evaporators onto a parylene substrate held at room temperature. For the transmission measurements, the attenuation of the soft-x-ray flux was determined by measuring the incident flux I_0 by using a highly transmitting Au grid, and measuring the transmitted flux with a Si photodiode. Simultaneously, the photocurrent drain on the sample was measured to determine the TEY spectra. A schematic of the experimental arrangement for the measurements as well as representative absorption spectra for an Fe thin film are shown in Fig. 1. To minimize the electric/magnetic field-dependent variations in the sample photocurrent, the measurements were made with the sample magnetized in remnance (95–100%), i.e., at zero applied magnetic field, with an extraction grid biased at a positive high voltage (typically 500–1000 V) placed near the front of the sample, away from the incident photons' path. At each photon energy, the TY and TEY intensities were measured for a fixed photon helicity, first after a positive field sufficient to saturate the moments of the film was applied and then turned off prior to signal collection, and then after a similar negative field pulse.

The determination of the helicity-dependent absorption cross sections require the measurements of the transmission spectra for two opposite magnetization directions, $I_{\pm}$, normalized to incident-photon flux, for the $L_{2,3}$ white lines of Fe as well as the corresponding substrate spectrum I_s, taken prior to the Fe deposition. The absorptivity of the film for the two photon helicities can easily be derived from these spectra:

$$\mu_{\pm} d = \mu_{\mathrm{tot}} \pm \frac{\delta\mu}{2} = \frac{1}{2}(\rho_+ + \rho_-) \pm \frac{1}{2}\frac{(\rho_+ - \rho_-)}{p_c \sin(\theta_i)} \qquad (1)$$

with $\rho_{\pm} = -\ln(I_{\pm}/I_s)$. $I_{\pm}$ is the transmission spectra for the Fe film plus the parylene substrate after normalization to the incident flux and I_s is the corresponding normalized spectrum for the uncovered parylene film. The first term in Eq. (1), μ_{tot}, is the total photoabsorption cross section, while the second term, $\delta\mu/2$, is the helicity-dependent contribution to the XAS, which must be corrected for the photon incidence angle θ_i, measured from surface normal and incomplete circular polarization p_c.

The determination of absolute photoabsorption cross sections in transmission is complicated by the presence of scattered light and second and higher-order light (that follows the same optical path as the first-order light) from the grating monochromators. Typically, the higher-order and scattered light contribute less than 1% to the total photon flux but may have a noticeable effect on the measured spectra near the absorption thresholds as they are less severely attenuated than the first-order light.[17–19] A simple method to determine the absolute cross sections is to normalize the measured spectra with a constant offset, to correct for any contributions from this unwanted light, and scale the pre-L_3 and post-L_2 edge regions of Fe to previously published absolute measurements.[20] The $\mu_{\pm}$ spectra, thus normalized, are shown in Fig. 1, along with published tabulated values[20] (that do not include near-edge autoionization resonances, i.e., white lines).

(2). *Saturation/Self-Absorption effects*. At the XAS white-line resonances, the photoabsorption cross sections increase markedly and the resulting photon penetration depth at that energy becomes comparable to the sampling volume (determined by the secondary electron escape length). As a result, at these white-line energies, the measured total decay-product yield intensity is reduced from the actual atomic absorption cross section. In addition, due to the significant difference between the respective mean-free paths of the incident photons at the L_3 and L_2 white lines, this reduction is larger at the L_3 energy, resulting in the distortion of the spectra. The situation is more severe for the MCD spectra. Since the helicity-dependent absorption cross sections at a white line are significantly different (up to 50% at the L_3 absorption edge), as the circular polarized radiation penetrates into the sample, the remaining flux is reduced more quickly for one helicity than the other, more strongly affecting the resultant MCD spectra.

The measured XAS signal at incident photon energy E, normalized to the incident flux, $S_x(E)/I_0(E)$, can be described by the following equation:[7,10,13,14]

$$\frac{S_x(E)}{I_0(E)} = \frac{A}{r^2} C_x \cdot D_x \int_0^d \frac{\mu_x(E,z)}{\cos\theta_i} \exp\left[-\int_0^z \left(\frac{\mu_{\mathrm{tot}}(E,z')}{\cos\theta_i} + \frac{\mu_{\mathrm{tot}}(E_x,z')}{\cos\theta_e} \right) dz' \right] dz, \qquad (2)$$

where the subscript x denotes a decay process within the detection energy window at E_x; A/r^2 is the solid angle subtended by the detector (active area, A, and distance from sample, r); C_x and D_x are the relative detection efficiency and decay mode probabilities, respectively; d is the film thickness; θ_i (θ_e) is the photon incidence (emission) angle measured from sample normal; and $\mu(E,z)$'s are the energy-*and* depth-dependent photoabsorption cross sections.

In the special case of uniform, homogeneous films $\mu(E,z) \rightarrow \mu(E)$ and, Eq. (2) reduces to

$$\frac{S_x(E)}{I_0(E)} = \frac{A}{r^2} \frac{C_x D_x \mu_x(E)}{\left(\mu_{\rm tot}(E) + \mu_{\rm tot}(E_x) \dfrac{\cos\,\theta_i}{\cos\,\theta_e}\right)} \times \left\{1 - \exp\left[-\left(\frac{\mu_{\rm tot}(E)}{\cos\,\theta_i} + \frac{\mu_{\rm tot}(E_x)}{\cos\,\theta_e}\right) d\right]\right\}. \quad (3)$$

For TEY, $\mu_x \rightarrow \mu_{\rm tot}$, since *all* absorption processes contribute to the TEY signal. Also, if one assumes that *all* electrons are collected, then $\mu_{\rm tot}(E_x)/\cos\,\theta_e \rightarrow \mu_e = 1/\xi$, where ξ is the phenomenological ''mean-escape depth'' for secondary electrons. Thus,

$$\frac{S_e(E)}{I_0(E)} \propto \frac{\mu_{\rm tot}(E)}{\left(\mu_{\rm tot}(E) + \dfrac{\cos\,\theta_i}{\xi}\right)} \left\{1 - \exp\left[-\left(\frac{\mu_{\rm tot}(E)}{\cos\,\theta_i} + \frac{1}{\xi}\right) d\right]\right\}. \quad (4)$$

There are a variety of criteria to monitor for the presence of saturation/self-absorption effects in indirect techniques. Since $\mu_{\rm tot}$ is much larger at the L_3 white line than the corresponding L_2 white line, one indication of the presence of saturation is a thickness- or angle-dependent variation in the $L_3{:}L_2$ white-line intensity ratio in XAS. As discussed above, an even larger variation in the $L_3{:}L_2$ white-line intensity ratio is present in the difference of the μ_+ and μ_- spectra, $\delta\mu$ $(=\mu_+ - \mu_-)$. Therefore, a more sensitive indicator for the presence of saturation effects is a thickness/angle-dependent variation in the $L_3{:}L_2$ intensity ratio of the MCD peak heights.

With the experimentally determined absolute cross sections presented above, the changes in the XAS spectra, $\mu_{\rm tot} = (\mu_+ + \mu_-)/2$, as a function of photon incidence angle can be calculated to quantitatively address the important issue of saturation/self-absorption effects manifested in TEY. Using a realistic mean-escape depth for secondary electrons, ξ, of 10 Å, and the film thickness, $d = 30$ Å, we can calculate the XAS and the corresponding MCD spectra at each incidence angle, shown in Fig. 2. Note that varying the film thickness would also result in a reduction in peak intensities (but functionally different).

A number of observations can immediately be made. First, as anticipated, even at normal photon incidence this thin film exhibits some saturation. Second, the XAS and MCD spectral shapes remain nearly unchanged for incidence angles less than $\sim 50°$ and thereafter visible saturation begins to occur and the white-line intensities begin to decrease rapidly. Third, although this is a relatively thin sample, saturation in XAS is expected even above the edge, indicating that normalizing the data from different measurements (e.g., samples with different thicknesses or different measurement geometries) to values above the edge can cause errors.

(3). *Comparison with experiment.* To verify the ideas presented in the previous section, we measured helicity-dependent photoabsorption cross sections from a thin 30 Å Fe film, measured simultaneously in TY and in TEY. To avoid the necessary complications due to sample-to-sample variations in a multiple-thickness measurement, the effective thickness of the thin film was changed by varying the incident-beam direction, similar to the calculations depicted in Fig. 2. The symbols in Fig. 3 show the TEY $L_3{:}L_2$ intensity ratios for XAS and MCD, normalized to the corresponding ratios for TY, as the photon incidence angle is varied from 15°–75° from sample normal, which corresponds to an effective thickness variation of 31–116 Å. Note that, as suggested by the calculations, the measured data exhibit saturation effects even near normal incidence and that for incidence angles of $\leqslant 50°$, the ratios do not change significantly. Starting at $\sim 50°$, both ratios start to deviate more rapidly away from unity. Note that the onset angle at which the saturation effect increases more rapidly will depend strongly on the actual thickness of the film and on the material used.

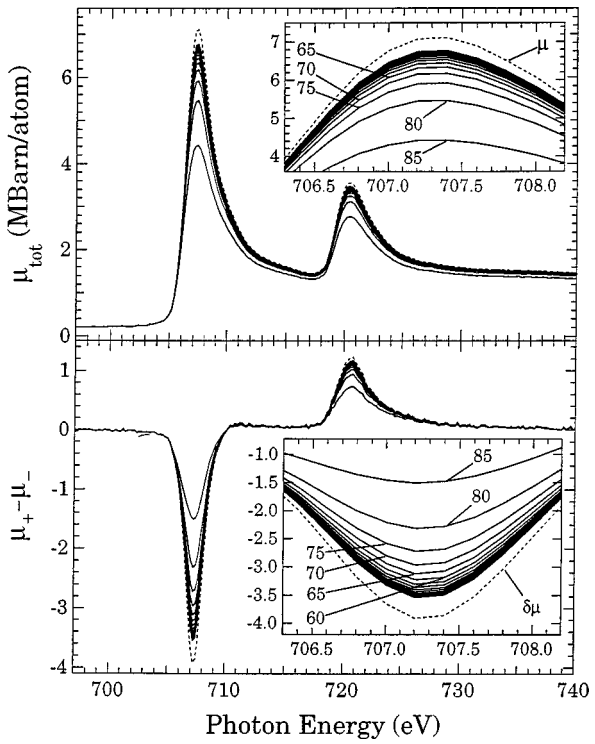

FIG. 2. Calculations showing the effect of saturation on XAS (top) and MCD (bottom) for a 30 Å Fe film with $\xi = 10$ Å. The unsaturated XAS, $\mu_{\rm tot}$ and MCD, $\delta\mu$, spectra measured in transmission are also shown for reference.

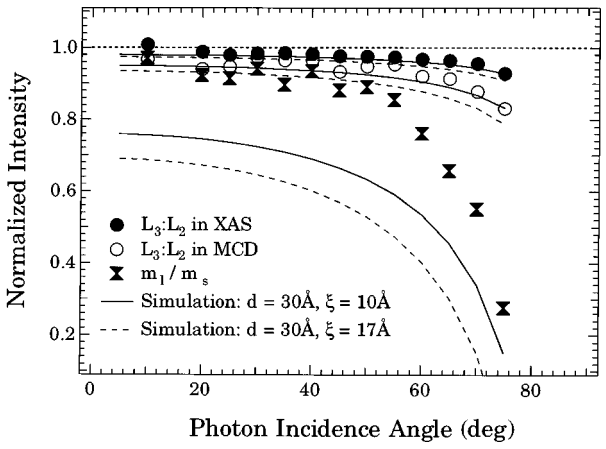

FIG. 3. Experimental TEY $L_3{:}L_2$ ratios for XAS and MCD as well as the m_l/m_s ratios for a 30 Å Fe film. The solid and dashed curves are the calculations as described in text with $\xi = 10$ and 17 Å, respectively.

Since, in MCD, the primary aim is to obtain quantitative information on the magnetic moment, it is imperative to assess the consequences of this saturation on the determined orbital and spin moments, m_l and m_s. While determined m_l and m_s are model-dependent,[4] their ratio, m_l/m_s, only depends on experimental quantities, i.e., on the relative sizes and signs of the L_3 and L_2 peaks in the MCD spectrum, and hence is of the more robust material parameters that can be obtained from the MCD data.[3,4,21] Note that, since saturation primarily affects the determined orbital moments, m_l, the changes in the m_l/m_s ratios will reflect the corresponding saturation in m_l. The m_l/m_s values obtained from TEY data, normalized to the values obtained from transmission, are also shown in Fig. 3. It is immediately apparent that while the deviation in the $L_3{:}L_2$ intensity ratios is small (but present) near normal-incidence angles, the resulting errors on the m_l/m_s values are significantly larger. More importantly, the deviation from unity increases much more rapidly than the corresponding deviation in the $L_3{:}L_2$ intensity ratios. This clearly demonstrates that the extent and the severity of the saturation effect can be strongly underestimated if one relies only on the $L_3{:}L_2$ intensity ratios as a criterion for saturation correction. Furthermore, since saturation is present at normal incidence, using normal-incidence spectra as ''reference'' for correcting the saturated spectra will also result in errors in the determined m_l/m_s values.

We can directly compare our experimental results with calculated values. The solid curves in Fig. 3 illustrate the calculated values for the three ''saturation criteria'' mentioned above, with the two free parameters in Eq. (4), i.e., d and ξ, set to 30 and 10 Å, respectively. The top solid curve was obtained by calculating the $L_3{:}L_2$ ratio for each XAS spectrum, after subtracting a continuum background.[4] The middle solid curve depicts the saturation in the $L_3{:}L_2$ peak intensity ratio in MCD, revealing that it is larger than in XAS and deviates from unity more rapidly. Finally, the bottom solid curve illustrates the corresponding saturation in the determined m_l/m_s ratio. Note that the film thickness (30 ± 5 Å) was determined by a combination of *in situ* absorption strength (in transmission) at the L_3 peak energy and *ex situ* x-ray fluorescence spectroscopy. On the other hand, ξ is largely unknown and was determined by comparing the simulated $L_3{:}L_2$ saturation to the measured ones.

Previously published results from related studies of Co and Ni single crystals or thin films indicate a value of 17–20 ±2 Å for ξ.[7–9] For reference, calculations using $\xi=17$ Å are also included in Fig. 3 (dashed curves) and show a worse agreement with the experiment. The lower value for ξ inferred in the present study can be understood by considering that Fe has a larger density of empty states of both spin characters that would result in enhanced inelastic electron scattering, and hence a smaller escape depth. More troubling, however, is the fact that the measured values for the m_l/m_s ratio are substantially less severely saturated than what the simulations find. In the calculations, the relative electron detection efficiency and decay mode probability were assumed to be energy *independent*, which is not true. In fact, if partial fluorescence yield can be used as an indicator, near strong white lines, the decay probabilities D, vary considerably with energy,[12] which may result in variations in TEY. Furthermore, the probability for electron escape and detection (related to the detection efficiency, C) may also depend on the incident-photon energy. If the energy dependence of these processes, which is largely unknown, is significant enough to measurably affect the TEY and MCD spectra, then the attempts at correcting measured spectra will be even more severely hampered. In addition to these energy-dependent processes, there may be spin-dependent processes that affect the measured TEY spectra. It is well known that the decay processes, which ultimately contribute to the TEY intensity, are spin-dependent.[12] This spin dependence of the decay and a possible spin dependence in the electron cascade process may result in a helicity-dependent mean-electron-escape depth $\xi_\pm$, further complicating attempts to model and correct for saturation.

This work was partially supported by the Office of Naval Research. Work done at National Synchrotron Light Source was supported by U.S. DOE, under Contract No. DE-AC02-76CH00016.

*Mailing address: c/o Brookhaven National Lab., Bldg. 510E, Upton, NY 11973.

†Present address: SRRC, Hsinchu Science-Based Industrial Park, Hsinchu 300, Taiwan, R.O.C.

[1] B. T. Thole *et al.*, Phys. Rev. Lett. **68**, 1943 (1992).

[2] P. Carra *et al.*, Phys. Rev. Lett. **70**, 694 (1993).

[3] R. Wu *et al.*, Phys. Rev. Lett. **73**, 1994 (1994).

[4] C. T. Chen *et al.*, Phys. Rev. Lett. **75**, 152 (1995).

[5] Y. Wu *et al.*, Phys. Rev. Lett. **69**, 2307 (1992).

[6] T. Böske *et al.*, Phys. Rev. B **49**, 4003 (1994).

[7] W. L. O'Brien *et al.*, Phys. Rev. B **50**, 12 672 (1994).

[8] J. Vogel *et al.*, Phys. Rev. B **49**, 3230 (1994).

[9] J. Hunter Dunn *et al.*, J. Phys. C **7**, 1111 (1995).

[10] Y. U. Idzerda *et al.*, Nucl. Instrum. Methods Phys. Res. A **347**, 134 (1994).

[11] F. M. F. de Groot *et al.*, Solid State Commun. **92**, 991 (1994).

[12] L.-C. Duda *et al.*, Phys. Rev. B **50**, 16 758 (1994).

[13] L. Tröger *et al.*, Phys. Rev. B **46**, 3283 (1992); S. Eisebitt *et al.*, *ibid.* **47**, 14 103 (1993).

[14] F. Yubero, S. Turchini, F. C. Vicentin, J. Vogel, and M. Sacchi, Solid State Commun. **93**, 25 (1995); F. C. Vicentin, S. Turchini, F. Yubero, J. Vogel, and M. Sacchi, J. Electron. Spectrosc. **74**, 187 (1995).

[15] C. T. Chen *et al.*, Rev. Sci. Instrum. **60**, 1616 (1989).

[16] C. T. Chen, Rev. Sci. Instrum. **63**, 1229 (1992).

[17] K. G. Tirsell *et al.*, in *X-ray and VUV interaction data bases, calculations and measurements*, edited by N. K. Del Grande, P. Lee, J. A. R. Samson, and D. Y. Smith (SPIE, New York, 1988), Vol. 911, p. 146.

[18] N. K. Del Grande *et al.*, in Ref. 17, p. 6.

[19] N. K. Del Grande, Phys. Scr. **41**, 110 (1990).

[20] B. L. Henke *et al.*, At. Data Nucl. Data Tables **54**, 181 (1993).

[21] V. Chakarian *et al.*, in *Synchrotron Radiation Techniques in Industrial, Chemical, and Materials Science*, edited by L. J. Terminello, K. L. D'Amico, and D. K. Shuh (Plenum, New York, 1995), p. 187.